Photonic-Assisted Regenerative Microwave Frequency Divider With a Tunable Division Factor

Shaochen Duan, Baohang Mo, Xudong Wang, Erwin H. W. Chan, *Senior Member, IEEE*, Xinhuan Feng, Bai-Ou Guan, and Jianping Yao, *Fellow, IEEE, Fellow, OSA*

***Abstract*—A photonic-assisted microwave frequency divider that is able to perform frequency division with a tunable division factor is presented. It is realized based on the regenerative approach in which frequency mixing and filtering operations are implemented using a dual-parallel Mach–Zehnder modulator (DPMZM) and an optical filter in an optoelectronic oscillator loop. The frequency division factor can be tuned by controlling the optical filter passband, the round-trip gain, and the time delay of the optoelectronic oscillator loop. The proposed approach is analyzed theoretically and verified experimentally. The phase conditions to achieve frequency division for a given division factor are analyzed. Experimental results demonstrate, for the first time, a photonic-assisted regenerative microwave frequency divider with a tunable frequency division factor of 2 to 6. One key application of a microwave frequency divider is to improve the phase noise performance of a microwave signal. In our experiment, the phase noise is reduced by 16.2 dB when a microwave signal is frequency divided by 6 times.**

***Index Terms*—Dual parallel Mach–Zehnder modulator, frequency division, microwave photonics, optical signal processing, optoelectronic oscillator.**

I. Introduction

FREQUENCY divider is a device that generates an output signal that is a subharmonic of the input signal. It is a fundamental building block in phase-locked loops, frequency synthesizers, serializers and deserializers, which are widely used for applications such as radar, communications and metrology [1]–[3]. Frequency dividers can also be used to improve the phase noise performance of a microwave or millimeter wave signal through frequency division.

Manuscript received January 20, 2020; revised June 21, 2020; accepted June 24, 2020. Date of publication June 29, 2020; date of current version October 1, 2020. This work was supported in part by the National Natural Science Foundation of China under Grant 61860206002 and Grant 61771221, and in part by Fundamental Research Funds for the Central Universities under Grant 21619403. *(Corresponding authors: Xudong Wang and Xinhuan Feng.)*

Shaochen Duan, Baohang Mo, Xudong Wang, Xinhuan Feng, and Bai-Ou Guan are with the Guangdong Provincial Key Laboratory of Optical Fiber Sensing and Communications, Institute of Photonics Technology, Jinan University, Guangzhou 510632, China (e-mail: duanshaochen@stu2016.jnu.edu.cn; mbh@stu2016.jnu.edu.cn; txudong.wang@email.jnu.edu.cn; eexhfeng@gmail.com; guanboo@yahoo.com).

Erwin H. W. Chan is with the College of Engineering, IT and Environment, Charles Darwin University, Darwin, NT 0909, Australia (e-mail: erwin.chan@cdu.edu.au).

Jianping Yao is with the Microwave Photonics Research Laboratory, School of Electrical Engineering and Computer Science,University of Ottawa, Ottawa, ON K1N 6N5, Canada (e-mail: jpyao@uottawa.ca).

Color versions of one or more of the figures in this article are available online at https://ieeexplore.ieee.org.

Digital Object Identifier 10.1109/JLT.2020.3005435

Traditional electronic frequency dividers are categorized by digital dividers and analog dividers. Digital frequency dividers are implemented using basic logic gates and flip-flops. To perform frequency division of a microwave signal, it is desired that the level of harmonics is low. A solution to have a low level of harmonics is to use analog frequency dividers. Analog frequency dividers are in general classified into two categories: injection locked and regenerative frequency dividers. An injection-locked frequency divider employs an oscillator whose center frequency is locked to a harmonic of the injected input signal. It can operate at a high frequency, up to tens of GHz. However, the bandwidth is very limited due to the resonance nature of the oscillator, making the divider operate at a fixed frequency or a tunable frequency with very small tunable range. A regenerative frequency divider is formed by a mixer and a low-pass filter in a feedback loop. Unlike an injection-locked frequency divider, a regenerative frequency divider does not support free-run, and an injected signal is needed to produce an output [4], [5]. It has a wide frequency tunable range, which is only limited by the system bandwidth. In addition to a wide frequency tunable range, it is also important for a frequency divider to have the ability to realize tunable frequency division factor without the need to modify the system configuration.

Recently, microwave frequency dividers implemented based on photonics techniques have been widely investigated thanks to the advantages such as wide bandwidth, immunity to electromagnetic interference, and integrability offered by photonics [6], [7]. A number of photonic-assisted microwave frequency dividers have been proposed. Many of them are realized using pure photonics approach, which relies on the nonlinear dynamics in a semiconductor device by injecting an optical signal into a semiconductor laser [8]–[10] or a semiconductor optical amplifier [11], [12]. The operating frequency of this type of frequency dividers is determined by the 3-dB bandwidth of the semiconductor devices, which is few tens of GHz. The frequency tunable range of these frequency dividers is several hundred MHz, which is quite limited. Recently, there are few reports on injection-locked and regenerative frequency dividers based on microwave photonics in which an optoelectronic oscillator (OEO) is employed. While a photonic-assisted injection-locked frequency divider with a tunable frequency division factor has been demonstrated, it has a small tunable bandwidth [3]. A photonic-assisted regenerative frequency divider has a wide bandwidth but the frequency division factor is fixed at 1/2 or 2/3 [13], [14].

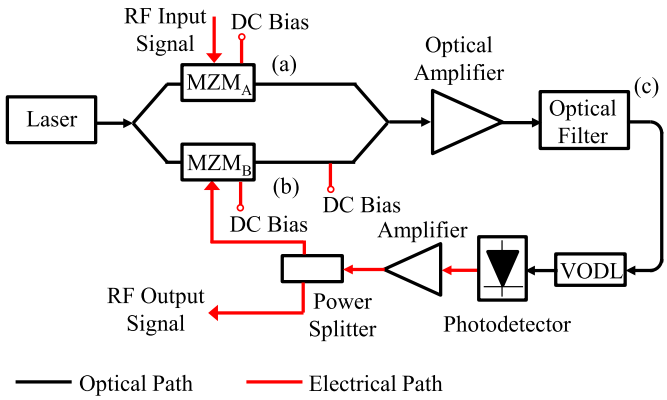

Fig. 1. Structure of the proposed photonic-assisted 1/*N* microwave frequency divider.

In this paper, we present a photonic-assisted regenerative microwave frequency divider that is capable to operate over a wide frequency tunable range with a tunable frequency division factor. It is realized based on an OEO loop incorporating a frequency mixer implemented by a dual-parallel Mach-Zehnder modulator (DPMZM), and an optical filter. The frequency division factor can be tuned by controlling the optical filter passband, the round-trip gain, and the time delay of the OEO loop. The conditions required for the proposed structure to generate a microwave signal with a frequency of 1/*N* times the input signal frequency are analyzed. Experimental demonstration is then performed, in which a tunable frequency division factor from 2 to 6 over a wide frequency range from 18 to 26 GHz is demonstrated. The results also demonstrate that the phase noise performance is improved when the frequency division factor is increased showing an excellent agreement between the experimental measurements and the theoretical prediction. This confirms the concept of divider-assisted low phase noise microwave signal generation, a promising solution for an OEO to further improve its phase noise performance.

II. Topology and Operation Principle

The structure of the proposed photonic-assisted 1/*N* microwave frequency divider is depicted in Fig. 1. It is similar to a conventional OEO [15]. The main difference is an optical filter, instead of an electrical bandpass filter, is incorporated into the loop. The frequency divider is operating based on the regenerative approach in which the input signal is mixed with the feedback signal via a DPMZM and a photodetector, and the unwanted optical frequency components are filtered out by an optical filter. The signal at the output of the photodetector that contains the 1/*N* frequency component is amplified and fed back to the DPMZM. In order to obtain an output signal with a frequency of 1/*N* times the input signal frequency, two conditions need to be satisfied, which are 1) the loop gain of the 1/*N* frequency component should be unity and 2) the total phase shift for the 1/*N* frequency component in one round trip is an integer multiple of 2π [1]. The loop gain and the phase shift can be controlled via adjusting the optical amplifier gain and the variable optical delay line (VODL) time delay. The key novelty of the proposed structure is that a tunable optical filter is used to select *N* number of sidebands at the output of the DPMZM to be detected by the photodetector such that an output signal with a frequency of 1/*N* times the input microwave signal frequency is generated.

With reference to Fig. 1, a continuous wave (CW) light from a laser source is modulated by a microwave signal at the DPMZM. The DPMZM consists of a main MZM and two sub-MZMs ($\mathrm{MZM_A}$ and $\mathrm{MZM_B}$) incorporated in each arm of the main MZM. $\mathrm{MZM_A}$ is driven by an input microwave signal with an angular frequency ω_{RF}. The input of $\mathrm{MZM_B}$ has *N*-1 frequency components with angular frequencies of $(N\text{-}m)\omega_{\mathrm{RF}}/N$ where *N* is the factor of frequency division and *m* is an integer from 1 to *N*-1. As an example, in the case of a divide-by-3 frequency divider, there are two frequency components with angular frequencies of $\omega_{\mathrm{RF}}/3$ and $2\omega_{\mathrm{RF}}/3$ applied to $\mathrm{MZM_B}$. These frequency components are originated from the noise in the system, which includes the laser RIN noise, the shot noise, the photodetector and electrical amplifier thermal noise, and the signal spontaneous beat noise. The generation of the $\omega_{\mathrm{RF}}/3$ and $2\omega_{\mathrm{RF}}/3$ frequency components from the broadband noise in the OEO loop is enabled by the phase condition which is achieved by controlling the OEO loop length. The details will be analyzed in Section III. The amplitudes of these frequency components increase as they circulate in the OEO loop when the gain condition is also satisfied. Both $\mathrm{MZM_A}$ and $\mathrm{MZM_B}$ are biased at the null point to maximize the amplitudes of the output first order sideband. The main MZM can be biased at any point with no effect on the frequency divider performance. For simplicity, the main MZM is biased at the quadrature point, so that the three DPMZM bias points are the same as those for realizing single sideband with suppressed carrier modulation [16]. This enables the use of a standard commercial DPMZM bias controller to stabilize the bias points. The signal at the output of the DPMZM, which consists of sidebands at $\omega_{\mathrm{c}} \pm \omega_{\mathrm{RF}}/N$, …, $\omega_{\mathrm{c}} \pm (N-1)\omega_{\mathrm{RF}}/N$ and $\omega_{\mathrm{c}} \pm \omega_{\mathrm{RF}}$, and a residual carrier at ω_c, is amplified by an optical amplifier and then sent to an optical filter. The passband of the optical filter is designed to filter out the upper sidebands and the residual carrier. The lower sidebands at ω_{c}-ω_{RF}/N, …, ω_{c}-$(N\text{-}1)\omega_{\mathrm{RF}}/N$ and ω_{c}-ω_{RF} are allowed to pass through the optical filter and then experience a time delay via a VODL. The beating at the photodetector will generate microwave frequency components at ω_{RF}/N, …, $(N\text{-}1)\omega_{\mathrm{RF}}/N$. These frequency components are amplified by an electrical amplifier before feeding back into $\mathrm{MZM_B}$ through a power splitter. The signal at the output of the power splitter contains a frequency component with an angular frequency of 1/*N* times the input microwave signal angular frequency.

The key advantages of implementing the proposed photonic-assisted microwave frequency divider are the wide tunable bandwidth and tunable frequency division factor. For example, an MZM with a 3-dB bandwidth of more than 100 GHz has been reported [17]. The bandwidth of the proposed microwave frequency divider is limited by the bandwidths of the electrical amplifier and the power splitter connected after the photodetector. The electrical amplifier and power splitter should have a bandwidth to cover a frequency range from f_{RF}/N to $(N-1)f_{\mathrm{RF}}/N$

in order to realize 1/*N* frequency division for an input microwave signal with a frequency of f_{RF}. Electrical amplifiers and power splitters with bandwidths more than 60 GHz are commercially available. Hence, the photonic-assisted 1/*N* frequency divider can be designed to have an upper operating frequency of 72 GHz for realizing 1/2 to 1/6 frequency division. The lower operating frequency for realizing all 1/2 to 1/6 frequency division is around 20 GHz. This is limited by the edge steepness of the magnitude response of the optical filter to ensure that the optical carrier is largely suppressed. The large tunable bandwidth from 20 to 72 GHz and tunable frequency division factor from 2 to 6 cannot be achieved by purely electronic frequency dividers. The photonic-assisted microwave frequency divider also has the potential to be integrated with significantly reduced size and power consumption. These advantageous features make photonic-assisted microwave frequency dividers an attractive candidate for applications where large bandwidth and tunable division factor are required.

III. Analysis

The electric field of the CW light from the laser source into the DPMZM shown in Fig. 1 is given by

$$E\left(t\right) = E_{in}e^{j\omega_c t} \tag{1}$$

where E_{in} is the amplitude of the electric field into the DPMZM and ω_{c} is the CW light angular frequency. The voltage of the microwave signal into the frequency divider is $V_{\mathrm{RF}}\sin(\omega_{\mathrm{RF}}t + \phi_{\mathrm{RF}})$ where V_{RF}, ω_{RF} and ϕ_{RF} are the amplitude, angular frequency, and phase of the input microwave signal, respectively. Hence, the electric field at the output of $\mathrm{MZM_A}$ is given by

$$\begin{aligned} E_{MZMA}\left(t\right) = \frac{1}{2\sqrt{2}}E_{in}e^{j\omega_c t}\left[\left(1-\gamma\right)J_0\left(\beta_{RF}\right)\right. \\ -\left(1+\gamma\right)J_1\left(\beta_{RF}\right)e^{-j\left(\omega_{RF}t+\phi_{RF}\right)} \\ \left.+\left(1+\gamma\right)J_1\left(\beta_{RF}\right)e^{j\left(\omega_{RF}t+\phi_{RF}\right)}\right] \end{aligned} \tag{2}$$

where $J_m(x)$ is the Bessel function of *m*th order of the first kind, $\beta_{\mathrm{RF}} = \pi V_{\mathrm{RF}}/V_\pi$, V_π is the switching voltage of the sub-MZMs and γ is a scaling factor between zero and one determined by the MZM extinction ratio [18]. This shows that at the output of $\mathrm{MZM_A}$, two sidebands are generated with a residual carrier, as shown in Fig. 2(a). In the case where the frequency divider is designed to realize 1/3 frequency division, as was discussed in Section II, the signal into $\mathrm{MZM_B}$ has two frequency components at angular frequencies of $\omega_{\mathrm{RF}}/3$ and $2\omega_{\mathrm{RF}}/3$. The voltage of the signal into $\mathrm{MZM_B}$ of the 1/3 frequency divider is $V_1\sin(\omega_{\mathrm{RF}}t/3 + \phi_1) + V_2\sin(2\omega_{\mathrm{RF}}t/3 + \phi_2)$ where V_1, V_2, ϕ_1 and ϕ_2 are the amplitude and phase terms of the frequency components at $\omega_{\mathrm{RF}}/3$ and $2\omega_{\mathrm{RF}}/3$, respectively. Hence the electric field at the output of $\mathrm{MZM_B}$ is given by

$$\begin{aligned} E_{MZMB}\left(t\right) = \frac{1}{2\sqrt{2}}E_{in}e^{j\omega_c t}\left[\left(1-\gamma\right)J_0\left(\beta_1\right)J_0\left(\beta_2\right)\right. \\ -\left(1+\gamma\right)J_1\left(\beta_1\right)J_0\left(\beta_2\right)e^{-j\left(\frac{\omega_{RF}}{3}t+\phi_1\right)} \\ +\left(1+\gamma\right)J_0\left(\beta_1\right)J_0\left(\beta_2\right)e^{j\left(\frac{\omega_{RF}}{3}t+\phi_1\right)} \\ -\left(1+\gamma\right)J_0\left(\beta_1\right)J_1\left(\beta_2\right)e^{-j\left(\frac{2\omega_{RF}}{3}+\phi_2\right)} \\ \left.+\left(1+\gamma\right)J_0\left(\beta_1\right)J_1\left(\beta_2\right)e^{j\left(\frac{2\omega_{RF}}{3}t+\phi_2\right)}\right] \end{aligned} \tag{3}$$

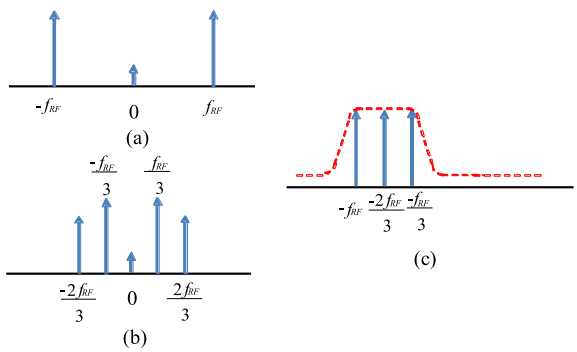

Fig. 2. Optical spectrum at the output of (a) $\mathrm{MZM_A}$, (b) $\mathrm{MZM_B}$ and (c) the optical filter. The frequencies of the spectral components in the optical spectrums are relative to the optical carrier frequency f_{c}. The red dashed line in (c) is the optical filter magnitude response.

where $\beta_1 = \pi V_1/V_\pi$ and $\beta_2 = \pi V_2/V_\pi$. Eq. (3) shows that at the output of $\mathrm{MZM_B}$, two pairs of sidebands are generated with a residual carrier, as shown in Fig. 2(b). Since the main MZM is biased at the quadrature point, the electric field at the output of the DPMZM can be written as

$$E_{DPMZM}\left(t\right) = \sqrt{\frac{t_{ff}}{2}}\left[E_{MZMA}\left(t\right) + E_{MZMB}\left(t\right)e^{j\frac{\pi}{2}}\right] \tag{4}$$

where t_{ff} is the DPMZM insertion loss. The passband of the optical filter is designed to pass the three lower sidebands while suppressing the three upper sidebands and the residual carrier. Hence the optical filter output electric field into the photodetector can be written as

$$\begin{aligned} E_o\left(t\right) = -\frac{\left(1+\gamma\right)}{4}\sqrt{t_{ff}}\sqrt{G_{OA}}E_{in}e^{j\omega_c t} \\ \cdot\left[J_1(\beta_{RF})e^{j\left(-\omega_{RF}t-\phi_{RF}\right)} + J_1(\beta_1)J_0(\beta_2)e^{j\left(\frac{-\omega_{RF}}{3}t-\phi_1+\frac{\pi}{2}\right)}\right. \\ \left.+J_0\left(\beta_1\right)J_1\left(\beta_2\right)e^{j\left(\frac{-2\omega_{RF}}{3}-\phi_2+\frac{\pi}{2}\right)}\right] \end{aligned} \tag{5}$$

where G_{OA} is the optical amplifier gain. Therefore, the signal at the output of the optical filter has three sidebands at ω_{c}-$\omega_{\mathrm{RF}}/3$, ω_{c}-$2\omega_{\mathrm{RF}}/3$ and ω_{c}-ω_{RF}, as shown in Fig. 2(c). By beating the two sidebands with frequencies at ω_{c}-$\omega_{\mathrm{RF}}/3$ and ω_{c}-$2\omega_{\mathrm{RF}}/3$ at the photodetector, a photocurrent at an angular frequency of $\omega_{\mathrm{RF}}/3$ is generated, which is given by

$$\begin{aligned} I_{\omega_{RF}/3,1} = \frac{\left(1+\gamma\right)^2}{8}t_{ff}G_{OA}P_{in}\Re J_1\left(\beta_1\right)J_0\left(\beta_2\right) \\ \times J_0\left(\beta_1\right)J_1\left(\beta_2\right)\cdot\cos\left(\frac{\omega_{RF}}{3}-\phi_1+\phi_2\right) \end{aligned} \tag{6}$$

where $\Re$ is the photodetector responsivity. By beating the sidebands at ω_c-$2\omega_{RF}/3$ and ω_c-ω_{RF} at the photodetector, a photocurrent at $\omega_{RF}/3$ is generated, which is given by

$$I_{\omega_{RF}/3,2} = \frac{(1+\gamma)^2}{8} t_{ff} G_{OA} P_{in} \Re J_1(\beta_{RF}) J_0(\beta_1) J_1(\beta_2) \cdot \cos\left(\frac{\omega_{RF}}{3} + \phi_{RF} - \phi_2 + \frac{\pi}{2}\right) \quad (7)$$

The phase conditions require that the 1/3 frequency component in one round trip should be in phase with the original 1/3 frequency component, i.e.,

$$\phi_2 - \phi_1 + \frac{\omega_{RF}}{3}\tau = \phi_1 + 2m\pi \quad (8)$$

$$\phi_{RF} - \phi_2 + \frac{\pi}{2} + \frac{\omega_{RF}}{3}\tau = \phi_1 + 2m'\pi \quad (9)$$

where τ is the round trip time delay, and m and m' are two integers. If the above phase conditions are satisfied, then the amplitude of the microwave signal at $\omega_{RF}/3$ into MZM_B can be written as

$$V'_{\omega_{RF}/3} = \frac{(1+\gamma)^2}{8\sqrt{2}} t_{ff} G_{OA} P_{in} \Re \sqrt{G_{Amp}} R_o J_1(\beta_2) \cdot \left[J_1(\beta_1) J_0(\beta_2) J_0(\beta_1) + J_1(\beta_{RF}) J_0(\beta_1)\right] \quad (10)$$

where G_{Amp} is the gain of the electrical amplifier and R_o is the photodetector load resistance. This shows that the amplitude of the signal at $\omega_{RF}/3$ into MZM_B can be controlled by the optical amplifier gain G_{OA}. Thus, the gain condition can be satisfied by adjusting the optical amplifier gain G_{OA}.

A photocurrent at $2\omega_{RF}/3$ is also generated at the output of the photodetector due to the beating between the two sidebands at ω_c-$\omega_{RF}/3$ and ω_c-ω_{RF}. It can be obtained from (5) and is given by

$$I_{2\omega_{RF}/3} = \frac{(1+\gamma)^2}{8} t_{ff} G_{OA} P_{in} \Re J_1(\beta_{RF}) J_1(\beta_1) J_0(\beta_2) \cdot \cos\left(\frac{2\omega_{RF}}{3} + \phi_{RF} - \phi_1 + \frac{\pi}{2}\right) \quad (11)$$

The amplitude of the microwave signal at $2\omega_{RF}/3$ into MZM_B is given by

$$V'_{2\omega_{RF}/3} = \frac{(1+\gamma)^2}{8\sqrt{2}} t_{ff} G_{OA} P_{in} \Re \sqrt{G_{Amp}} R_o J_1(\beta_{RF}) J_1(\beta_1) J_0(\beta_2) \quad (12)$$

Note from (10) that, even without the input microwave signal at ω_{RF}, a signal at $\omega_{RF}/3$ can be generated at the frequency divider output due to the beating between the ω_c-$\omega_{RF}/3$ and ω_c-$2\omega_{RF}/3$ sidebands at the photodetector. However, from (12), the signal at $2\omega_{RF}/3$ and hence the sideband at ω_c-$2\omega_{RF}/3$, cannot be generated when the input microwave signal at ω_{RF} is absent. This is the reason why the input signal at ω_{RF} is necessary for the proposed photonic-assisted frequency divider to generate a divide-by-*N* output signal. The total phase shift of the signal at $2\omega_{RF}/3$ in one round trip needs to be an integer multiple of 2π, i.e.,

$$\phi_{RF} - \phi_1 + \frac{\pi}{2} + \frac{2\omega_{RF}}{3}\tau - \phi_2 = 2m''\pi \quad (13)$$

in order for the signal amplitude to build up as the number of circulations increases, so that a divide-by-3 frequency component can be obtained at the frequency divider output. Note that m'' in (13) is an integer. Combining the phase conditions in (8), (9) and (13), we obtain the following conditions

$$\phi_{RF} - 3\phi_1 + \frac{\pi}{2} = 2m'''\pi \quad (14)$$

$$\frac{\omega_{RF}}{3}\tau = 2m''''\pi \quad (15)$$

where m''' and m'''' are integers. The above analysis also applies to frequency division of 1/4, 1/5, …, and 1/*N*. It reveals that the 1/*N* frequency component at the output of a 1/*N* frequency divider is formed by the sum of *N*-1 beating terms and the phase conditions required for realizing 1/*N* frequency division are given by

$$\phi_{RF} - N\phi_1 + \frac{\pi}{2} = 2m'''\pi \quad (16)$$

$$\frac{\omega_{RF}}{N}\tau = 2m''''\pi \quad (17)$$

Eq. (16) shows the relationship between the phase ϕ_{RF} of the microwave signal into MZM_A and the phase ϕ_1 of the 1/*N* frequency component into MZM_B. Note that the 1/*N* frequency component is originated from the noise in the system and the noise has a random phase. Therefore, the 1/*N* frequency component always has a phase that satisfies the phase condition given in (16). Eq. (17) is important as it indicates that, for a given input frequency and a given factor of frequency division, the round-trip time τ needs to be controlled for the proposed structure to generate an output signal with a frequency of 1/*N* times the input microwave signal frequency.

According to the above analysis, three system parameters need to be controlled in order for the 1/*N* frequency divider to switch from one frequency division factor to another. The three system parameters are the optical amplifier gain G_{OA}, the VODL time delay τ, and the optical filter passband frequency. The values of these parameters can be controlled via a computer to enable 1/*N* frequency division to be obtained for a different input frequency. The phase noise at the output of the proposed 1/*N* frequency divider is given by

$$10\log_{10}\left[S_{\phi,out}(f)\right] = 10\log_{10}\left[S_{\phi,RFin}(f)/N^2\right] + 10\log_{10}\left[S_{\phi,OEO}(f)\right] \quad (18)$$

where $S_{\phi,RFin}(f)$ and $S_{\phi,OEO}(f)$ are the phase noise of the input microwave signal and that of the OEO loop, respectively. The phase noise of the OEO loop is the sum of the phase noise generated by the components in the OEO loop divided by the square of the frequency division factor [19]. If $S_{\phi,OEO}(f) << S_{\phi,RFin}(f)$, which is usually true since an OEO loop can be designed to have an ultra-low phase noise, the phase noise of the frequency divided signal will be determined uniquely by the phase noise of the input microwave signal, which is equal to the phase noise of the input microwave signal minus $20\log_{10}N$ (dB).

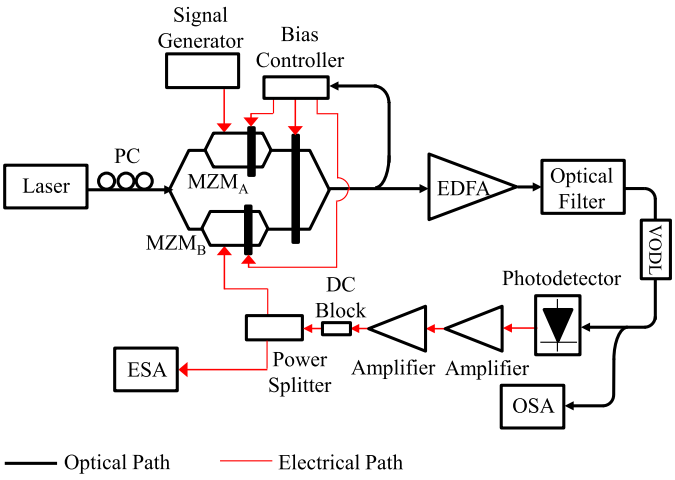

Fig. 3. Experimental setup of the proposed photonic-assisted microwave frequency divider.

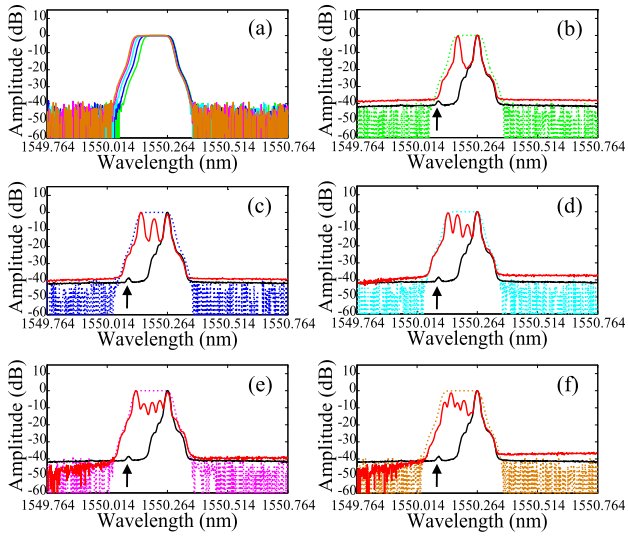

Fig. 4. (a) Normalized optical filter magnitude response for realizing 1/2 (green), 1/3 (blue), 1/4 (light blue), 1/5 (pink) and 1/6 (brown) frequency division. Normalized open loop (black line) and closed loop (red line) output optical spectrums together with the corresponding optical filter magnitude response (dotted line) for (b) 1/2, (c) 1/3, (d) 1/4, (e) 1/5 and (f) 1/6 frequency division. The arrows in (b)-(f) indicate the optical carrier.

IV. Experimental Results

An experiment is performed based on the setup shown in Fig. 3 to verify the operation of the photonic-assisted microwave frequency divider. A CW light from a laser source (IDPhotonics CoBriteDX$_1$) operating at 1550.1 nm and 15.5 dBm is launched into a DPMZM (EOSpace IQ-0D6V-35) through a polarization controller (PC). One of the sub-MZMs (MZM$_A$) inside the DPMZM is driven by a microwave signal from a microwave signal generator. The microwave signal frequency is 20 GHz and its power is 15 dBm. 1% of the DPMZM output optical power is coupled out to a bias controller (PlugTech MBC-IQ-01) to stabilize the DPMZM bias points at the null (MZM$_A$), null (MZM$_B$) and quadrature (main MZM) points. An erbium-doped fiber amplifier (EDFA) (Max-ray Photonics EDFA-BA-20-B) is used to control the output optical signal power to ensure that the gain condition can be satisfied. This is followed by an optical filter (Alnair Labs BVF-300CL), which has a sharp edge roll-off of 1500 dB/nm and a continuously tunable center frequency and bandwidth. A VODL (General Photonics MDL-002) is used to control the OEO loop time delay to ensure the phase condition given in (17) can be satisfied for a different input signal frequency and a different frequency division factor. This VODL has a built-in DC motor to provide a fine delay resolution of 1 fs over 0 to 560 ps delay range. A 5% coupling ratio optical coupler is connected to the optical filter output to couple a small amount of the output optical signal out of the OEO loop for examining the open and closed loop optical spectrums using an optical spectrum analyzer (OSA). The output optical signal is detected by a 50-GHz bandwidth photodetector (U2t XPDV2120RA). The electrical signal at the output of the photodetector is amplified by two wideband electrical amplifiers, which have a gain of 21 dB (Centellax OA4SMM5) and 26 dB (SHF 806E). A DC block is connected after the electrical amplifiers to prevent a DC component generated by the photodetector into MZM$_B$ which may alter the bias point. The amplified electrical signal is split into two via a 1–40 GHz bandwidth power splitter. One of the outputs is fed back to MZM$_B$ inside the DPMZM and the other is sent to an electrical spectrum analyzer (ESA) (Keysight N9020B) with the setting of 100 kHz resolution bandwidth and 10 kHz video bandwidth. The length of the OEO loop is around 36 m. This is very short compared to the loop length of the conventional OEO reported in [15], which has a long loop length of 1 km. It is known that a longer loop length will enable an OEO to have a higher Q factor, making the phase noise smaller [15].

The passband of the optical filter is adjusted to let N number of sidebands at the optical frequencies between f_c-20/N GHz and f_c-20 GHz to pass through the optical filter for realizing 1/N frequency division. Fig. 4(a) shows the magnitude responses of the optical filter required for the frequency divider to generate a 1/2 to 1/6 frequency components. It can be seen from Fig. 4, as the frequency division factor increases, the left edge of the magnitude response of the optical filter moves further to the left while the right edge remains the same. This allows the sideband at f_c-20/N GHz to pass through the optical filter. Fig. 4(b)-(f) shows the optical spectrums measured at the output of the optical coupler. As can be seen, when the OEO loop is open, there is only one sideband at the frequency of 20 GHz away from the optical carrier. This sideband comes from MZM$_A$ driven by the input 20 GHz signal. The optical carrier is around 40 dB below the sideband at f_c-20 GHz. When the OEO loop is closed and after properly adjusting the EDFA gain and the VODL time delay to satisfy the phase condition given in (17), sidebands at frequencies of $-20/N$ GHz to $-20(N\text{-}1)/N$ GHz away from the optical carrier are generated. By beating these sidebands with the sideband at f_c-20 GHz at the photodetector, an output signal with frequency components at 20/N GHz to 20(N-1)/N GHz are generated. Fig. 5 shows the input 20 GHz microwave signal spectrum and the photonic-assisted microwave frequency divider output spectrums for different frequency division factors from 2 to 6. Note that the phase condition for realizing

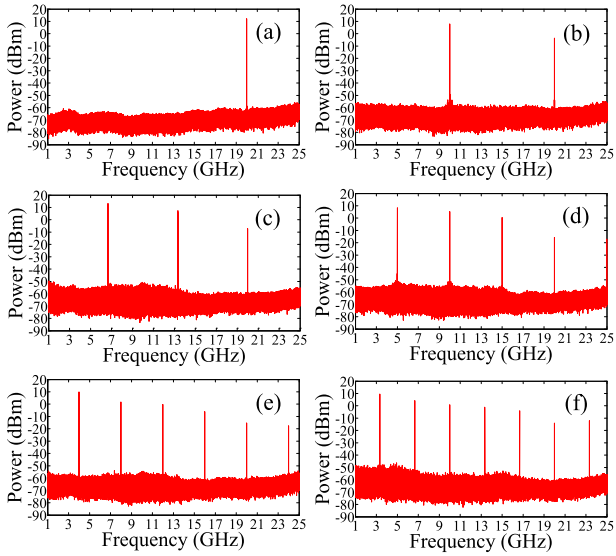

Fig. 5. (a) Electrical spectrum of the microwave signal into MZM_A. Photonic-assisted microwave frequency divider output electrical spectrums for realizing (b) 1/2, (c) 1/3, (d) 1/4, (e) 1/5 and (f) 1/6 frequency division.

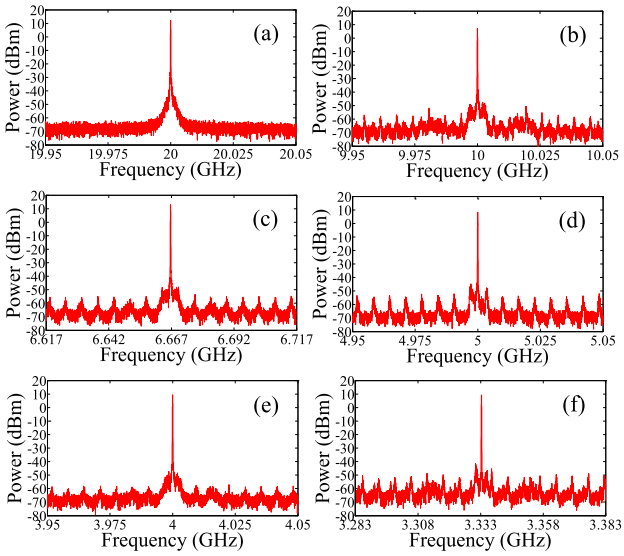

Fig. 6. (a) Electrical spectrum of the microwave signal into MZM_A measured in a 100 MHz span around the signal frequency. Photonic-assisted microwave frequency divider output electrical spectrums for realizing (b) 1/2, (c) 1/3, (d) 1/4, (e) 1/5 and (f) 1/6 frequency division measured in a 100 MHz span around the 1/*N* signal frequency.

1/6 frequency division also satisfies the 1/2 and 1/3 frequency division phase condition requirement. Compared to 1/2 and 1/3 frequency division, a wider optical filter passband is needed for 1/6 frequency division. When the optical filter passband is wider enough to cover the sidebands at angular frequencies of $\omega_{\mathrm{RF}}/6$ to ω_{RF} away from the optical carrier, all 1/2, 1/3 and 1/6 frequency components are generated. Fig. 5(f) shows that the 1/6 frequency component has a higher amplitude because it is formed by beating more sidebands at the photodetector, compared to the 1/2 and 1/3 frequency components. Fig. 6 shows the detailed section of the spectrum within 100 MHz span around the input microwave signal frequency at 20 GHz and around the output signal frequency at 20/*N* GHz. It can be seen clearly from Fig. 6 that the output signal contains a 1/*N* frequency component at exactly 20/*N* GHz, and the signal-to-spur ratio for all frequency division factors from 2 to 6 are larger than 50 dB.

Theoretically, a frequency division factor of larger than 6 can be obtained by increasing the optical filter passband width. However, as the frequency division factor increases, the number of sidebands increases. The optical amplifier inside the OEO loop needs to have a gain spectrum to simultaneously amplify all the sidebands so that their amplitudes can be built up as they circulate in the OEO loop. Furthermore, the edges of the optical filter magnitude response need to be sharp enough to ensure the optical carrier and the unwanted sidebands are largely suppressed.

It is found that there is no output signal presence at the frequency divider output when the input 20 GHz microwave signal is removed from the system, which demonstrates that the frequency divider is operating based on the regenerative approach. Note that Fig. 5 shows the output of the frequency divider has frequency components at and above the input signal frequency of 20 GHz. They are 20–30 dB below the 1/*N* frequency component and are the harmonics and third-order intermodulation distortion components generated by the nonlinearity of the two electrical amplifiers used in the system. It is found from the experiment that, taking the signal from the output of the first electrical amplifier as the frequency divider output, the amplitudes of the output frequency components at and above the input signal frequency will be more than 50 dB lower than that of the 1/*N* frequency component. Another solution to reduce those unwanted frequency components is to use linear electrical amplifiers with less nonlinearity.

The stability of the frequency divider is also evaluated, which is done by measuring the power of the generated 1/*N* frequency component over 10 minutes. The power fluctuations during the measurement period are less than 0.3 dB, which indicates that the frequency divider has good stability. In order to verify the phase condition given in (17), we observe the generated 1/3 frequency component using the ESA while tuning the time delay generated by the miniature motorized VODL. It is found that the 1/3 frequency component is generated for every 150 ps time delay introduced by the VODL. This agrees with the equation, given by

$$\tau_{VODL2} - \tau_{VODL1} = \frac{N}{f_{RF}} \tag{19}$$

where τ_{VODL1} and τ_{VODL2} are two different time delays introduced by the VODL in the OEO loop to satisfy the phase condition given by (17) in obtaining 1/*N* frequency division.

The phase noise performance of the divide-by-*N* output signal generated by the photonic-assisted microwave frequency divider is also evaluated, which is done by measuring the single-sideband phase noise using the ESA. Fig. 7 shows the phase noise spectrums of the 20/*N* GHz frequency divided signals and the input 20 GHz microwave signal. As can be seen, the phase noise of the input 20 GHz microwave signal is −90.53 dBc/Hz at a

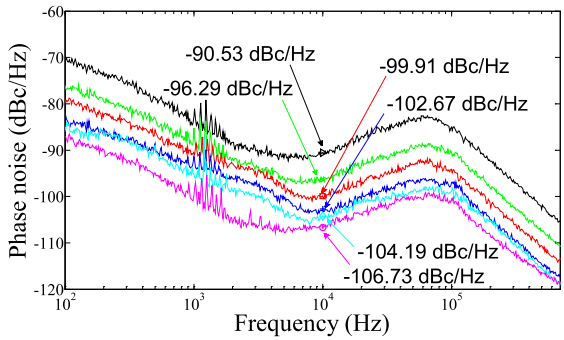

Fig. 7. Phase noise spectrum of the input 20 GHz microwave signal from the microwave signal generator (black). Phase noise spectrums of the frequency divider output signal at the frequency of 20/2 = 10 GHz (green), 20/3 = 6.67 GHz (red), 20/4 = 5 GHz (blue), 20/5 = 4 GHz (light blue) and 20/6 = 3.33 GHz (pink).

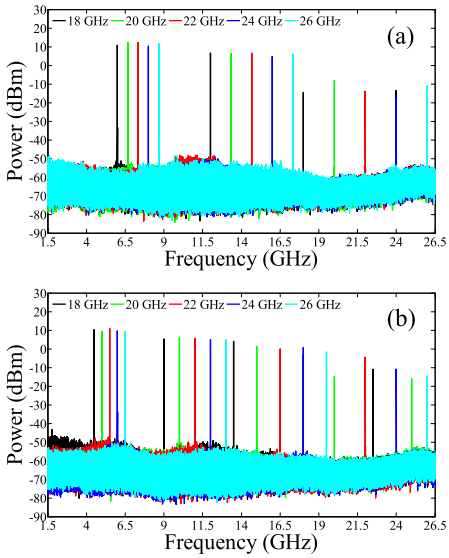

Fig. 8. Photonic-assisted microwave frequency divider output electrical spectrums for (a) 1/3 and (b) 1/4 frequency division, and a different input microwave signal frequency.

10-kHz frequency offset, while the phase noise of the 20/*N* GHz frequency divided signals are −96.29 dBc/Hz, −99.91 dBc/Hz, −102.67 dBc/Hz, −104.19 dBc/Hz and −106.73 dBc/Hz for the frequency division factors of 2, 3, 4, 5 and 6, respectively. This shows a 5.8 dB, 9.4 dB, 12.1 dB, 13.7 dB, and 16.2 dB improvement in the phase noise performance when increasing the frequency division factor from 2 to 6, respectively. This again agrees with the theoretical prediction of phase noise reduction given by $20\log_{10}(N)$ where N is the frequency division factor. This demonstrates the concept of phase noise reduction by frequency division.

The frequency tuning of the proposed photonic-assisted microwave frequency divider is also studied. To do so, we tune the frequency of the input microwave signal from 18 to 26 GHz with a step of 2 GHz. Fig. 8 shows the electrical spectrums of the generated frequency divided microwave signals. Note that during the tuning, the VODL and the optical filter are tuned to satisfy the phase conditions required for the realization of 1/3 and 1/4 frequency division. As can be seen less than 2 dB and 1.5 dB variations in amplitude of the generated 1/3 and 1/4 frequency components are resulted when the input microwave signal frequency is tuned from 18 to 26 GHz. The unwanted frequency components can be suppressed by using a low pass filter connected at the output of the frequency divider.

V. Conclusion

A photonic-assisted microwave frequency divider has been presented and its operation has been evaluated. The key contribution of this work is a frequency divider that is capable of tuning the frequency division factor and can operate at a wide frequency tunable range. The proposed frequency divider was studied theoretically and evaluated experimentally. The experimental results showed that the proposed photonic-assisted regenerative microwave frequency divider was able to realize frequency division with a tunable division factor from 2 to 6. The phase conditions obtained from the analysis were also verified experimentally. The phase-noise performance improvement when increasing the division factor was also verified by the experiment. The results showed that when increasing the frequency division factor from 2 to 6, a phase noise reduction of 5.8 dB, 9.4 dB, 12.1 dB, 13.7 dB and, 16.2 dB was achieved. Frequency tuning over a wide frequency range from 18 to 26 GHz was also demonstrated.

References

[1] A. Q. Safarian and P. Heydari, "A study of high-frequency regenerative frequency dividers," in *Proc. 2005 IEEE Int. Symp. Circuits Syst.*, 2005, pp. 2695–2698.

[2] K. Sengupta, T. K. Bhattacharyya, and H. Hashemi, "A nonlinear transient analysis of regenerative frequency dividers," *IEEE Trans. Circuits Syst. I, Reg. Papers*, vol. 54, no. 12, pp. 2646–2660, Dec. 2007.

[3] Y. Xu *et al.*, "Injection-locked millimeter wave frequency divider utilizing optoelectronic oscillator based optical frequency comb," *IEEE Photon. J.*, vol. 11, no. 3, pp. 1–8, May 2019.

[4] R. L. Miller, "Fractional-frequency generators utilizing regenerative modulation," *Proc. IRE*, vol. 27, no. 7, pp. 446–457, Jul. 1939.

[5] S. Verma, H. R. Rategh, and T. H. Lee, "A unified model for injection-locked frequency dividers," *IEEE J. Solid-State Circuits*, vol. 38, no. 6, pp. 1015–1027, Jun. 2003.

[6] R. A. Minasian, E. H. W. Chan, and X. Yi, "Microwave photonic signal processing," *Opt. Express*, vol. 21, no. 19, pp. 22918–22936, Oct. 2013.

[7] J. Yao, "Microwave Photonics," *J. Lightw. Technol.*, vol. 27, no. 3, pp. 314–335, Feb. 2009.

[8] S. C. Chan and J. M. Liu, "Microwave frequency division and multiplication using an optically injected semiconductor laser," *IEEE J. Quantum Electron.*, vol. 41, no. 9, pp. 1142–1147, Aug. 2005.

[9] L. Fan *et al.*, "Subharmonic microwave modulation stabilization of tunable photonic microwave generated by period-one nonlinear dynamics of an optically injected semiconductor laser," *J. Lightw. Technol.*, vol. 32, no. 23, pp. 4660–4666, Oct. 2014.

[10] M. Zhang, T. Liu, A. Wang, J. Zhang, and Y. Wang, "All-optical clock frequency divider using Fabry–Perot laser diode based on the dynamical period-one oscillation," *Opt. Comm.*, vol. 284, no. 5, pp. 1289–1294, Mar. 2011.

[11] A. E. Kelly, R. J. Manning, A. J. Poustie, and K. J. Blow, "All-optical clock division at 10 and 20 GHz in a semiconductor optical amplifier based nonlinear loop mirror," *Electron. Lett.*, vol. 34, no. 13, pp. 1337–1339, Jun. 1998.

[12] W. Zhang, J. Sun, J. Wang, X. Zhang, and D. Huang, "Optical clock division based on dual-wavelength mode-locked semiconductor fiber ring laser," *Opt. Express*, vol. 16, no. 15, pp. 11231–11236, Jul. 2008.

[13] S. Liu, K. Lv, J. Fu, L. Wu, W. Pan, and S. Pan, "Wideband microwave frequency division based on an optoelectronic oscillator," *IEEE Photon. Technol. Lett.*, vol. 31, no. 5, pp. 389–392, Jan. 2019.
[14] H. Zhou *et al.*, "Broadband two-thirds photonic microwave frequency divider," *Electron. Lett.*, vol. 55, no. 21, pp. 1141–1143, Oct. 2019.
[15] X. S. Yao and L. Maleki, "Optoelectronic microwave oscillator," *J. Opt. Soc. America B*, vol. 13, no. 8, pp. 1725–1735, Aug. 1996.
[16] K. Higuma, S. Oikawa, Y. Hashimoto, H. Nagata, and M. Izutsu, "X-cut lithium niobate optical single-sideband modulator," *Electron. Lett.*, vol. 37, no. 8, pp. 515–516, Apr. 2001.
[17] X. Wang, P. O. Weigel, J. Zhao, M. Ruesing, and S. Mookherjea, "Achieving beyond-100-GHz large-signal modulation bandwidth in hybrid silicon photonics Mach–Zehnder modulators using thin film lithium niobate," *APL Photon.*, vol. 4, Sep. 2019, Art. no. 096101.
[18] H. Kim and A. H. Gnauck, "Chirp characteristics of dual-drive Mach-Zehnder modulator with a finite DC extinction ratio," *IEEE Photon. Technol. Lett.*, vol. 14, no. 3, pp. 298–300, Aug. 2002.
[19] E. S. Ferre-Pikal and F. L. Walls, "Microwave regenerative dividers with low phase noise," in *Proc. IEEE MTT-S Int. Microw. Symp. Dig.*, 1998, pp. 1447–1450.

Shaochen Duan is currently a final year student pursuing the B.Sc. degree in optical engineering with in the Institute of Photonics Technology, Jinan University, China. His research interest is microwave photonic signal processing.

Baohang Mo is currently a final year student pursuing the B.Sc. degree in optical engineering with the Institute of Photonics Technology, Jinan University, China. His research interest is microwave photonic signal processing.

Xudong Wang received the B.E. degree in electrical engineering from Dalian University of Technology, Dalian, China, in 2007, the M.E. and Ph.D. degrees from the University of Sydney, Australia, in 2008 and 2014, respectively. He is currently an Associate Professor with the Institute of Photonics Technology, Jinan University, China. His research interest is microwave photonic signal processing.

Erwin H. W. Chan (Senior Member, IEEE) received the B.Sc., B.Eng. (Hons.) and Ph.D. degrees from the University of Sydney, Australia, in 1998, 2000 and 2005, respectively. He is currently an Associate Professor with the College of Engineering, IT and Environment, Charles Darwin University, Australia. He was a Senior Research Fellow and an External Lecturer with the University of Sydney from 2005 to 2014. His research interests include microwave photonics, optical telecommunications, optical signal processing, and photonic and microwave technology. He has published over 130 papers in international refereed journals and conferences, and has carried out consulting work with industry. Dr Chan has been a member of the Technical Program Committee of the Conference on Laser and Electro-optics (CLEO). He was the recipient of the University of Sydney Early Career Development Award, and the Australian Postdoctoral Fellowship, awarded by the Australian Research Council.

Xinhuan Feng received the B.Sc degree in physics from Nankai University in 1995, and obtained the M.Sc and Ph.D degrees in 1998 and 2005, respectively from the Institute of Modern Optics, Nankai University, China. From 2005 to 2008, she worked as a Postdoctoral Fellow at Photonics Research Centre of the Hong Kong Polytechnic University. Since March 2009, she has been with the Institute of Photonics Technology, Jinan University, China. Her research interests include various fiber active and passive devices and their applications, and microwave photonic signal processing.

Bai-Ou Guan received the B.Sc. degree in applied physics from Sichuan University, Chengdu, China, in 1994, and the M.Sc. and Ph.D. degrees in optics from Nankai University, Tianjin, in 1997 and 2000, respectively. From 2000 to 2005, he was with the Department of Electrical Engineering, the Hong Kong Polytechnic University, Hong Kong, first as a Research Associate, then as a Postdoctoral Research Fellow. From 2005 to 2009, he was with School of Physics and Optoelectronic Engineering, Dalian University of Technology, Dalian, as a Full Professor. In 2009, he joined Jinan University, Guangzhou, where he founded the Institute of Photonics Technology. His current research interests include fiber optic devices and technologies, optical fiber sensors, biomedical photonic sensing and imaging, and microwave photonics. He has authored and coauthored more than 230 technical papers in peer-reviewed international journals and presented more than 30 invited talks at major international conferences. He received the Distinguished Young Scientist Grant from Natural Science Foundation of China (NSFC) in 2012. He is a member of IEEE and OSA, and has served as the General Chair/Co-Chair, Technical Program Committee or Subcommittee Chair/Co-Chair for over 10 international conferences.

Jianping Yao (Fellow, IEEE, Fellow, OSA) received the Ph.D. degree in electrical engineering from the Universit´e de Toulon et du Var, Toulon, France, in December 1997. He is a Distinguished University Professor and University Research Chair with the School of Electrical Engineering and Computer Science, University of Ottawa, Ottawa, ON, Canada. From 1998 to 2001, he was with the School of Electrical and Electronic Engineering, Nanyang Technological University, Singapore, as an Assistant Professor. In December 2001, he joined the School of Electrical Engineering and Computer Science, University of Ottawa as an Assistant Professor, where he was promoted to an Associate Professor in May 2003, and a Full Professor in May 2006. He was appointed the University Research Chair in Microwave Photonics in 2007. In June 2016, he was conferred the title of Distinguished University Professor of the University of Ottawa. From July 2007 to June 2010 and from July 2013 to June 2016, he was the Director of the Ottawa-Carleton Institute for Electrical and Computer Engineering. He has authored or co-authored more than 560 research papers including more than 330 papers in peer-reviewed journals and more than 230 papers in conference proceedings. Prof. Yao is the Editor-in-Chief of IEEE PHOTONICS TECHNOLOGY LETTERS, a Topical Editor of Optics Letters, an Associate Editor of Science Bulletin, a Steering Committee Member of the IEEE JOURNAL OF LIGHTWAVE TECHNOLOGY, and an Advisory Editorial Board Member of *Optics Communications*. He was a Guest Editor of a Focus Issue on Microwave Photonics in *Optics Express* in 2013, a Lead-Editor of a Feature Issue on Microwave Photonics in Photonics Research in 2014, and a Guest Editor of a Special Issue on Microwave Photonics in the IEEE JOURNAL OF LIGHTWAVE TECHNOLOGY, in 2018. He is currently the Chair of the IEEE Photonics Ottawa Chapter and is the Technical Committee Chair of IEEE MTT-3 Microwave Photonics. He was a member of the European Research Council Consolidator Grant Panel in 2016, the Qualitative Evaluation Panel in 2017, and a member of the National Science Foundation Career Awards Panel in 2016. He was also a chair of a number of international conferences, symposia, and workshops, including the Vice Technical Program Committee (TPC) Chair of the 2007 IEEE Topical Meeting on Microwave Photonics, TPC Co-Chair of the 2009 and 2010 Asia-Pacific Microwave Photonics Conference, TPC Chair of the High-Speed and Broadband Wireless Technologies Subcommittee of the IEEE Radio Wireless Symposium 2009-2012, TPC Chair of the Microwave Photonics Subcommittee of the IEEE Photonics Society Annual Meeting 2009, TPC Chair of the 2010 IEEE Topical Meeting on Microwave Photonics, General Co-Chair of the 2011 IEEE Topical Meeting on Microwave Photonics, TPC Co-Chair of the 2014 IEEE Topical Meetings on Microwave Photonics, and General Co-Chair of the 2015 and 2017 IEEE Topical Meeting on Microwave Photonics. He was also a committee member for a number of international conferences, such as IPC, OFC, BGPP, and MWP. He is the recipient of the 2005 International Creative Research Award of the University of Ottawa, the 2007 George S. Glinski Award for Excellence in Research, a Natural Sciences and Engineering Research Council of Canada Discovery Accelerator Supplements Award in 2008, an inaugural OSA Outstanding Reviewer Award in 2012, and the Award for Excellence in Research 2017-2018 of the University of Ottawa. He was one of the top ten reviewers of IEEE/OSA JOURNAL OF LIGHTWAVE TECHNOLOGY (2015–2016). He was an IEEE MTT-S Distinguished Microwave Lecturer for 2013–2015. He is a registered Professional Engineer of Ontario. He is a Fellow of the Optical Society of America, the Canadian Academy of Engineering, and the Royal Society of Canada.